Chemistry & Biology Interface, 2019, 9, 6, 285-296

RESEARCH PAPER ISSN: 2249 –4820

CHEMISTRY & BIOLOGY INTERFACE

An official Journal of ISCB, Journal homepage; www.cbijournal.com

A Comparative Binding Study of β-Carboline Derivatives with Nucleic Acids in the Presence and Absence of the Gold Nanoparticles: Spectroscopic and Molecular Docking

Monika Yadav[1], Srashti Bhardwaj[1], Jaybir Singh[2], Prem Man Singh Chauhan[3] and Surat Kumar*[1]

[1]Department of Chemistry, Faculty of Science, Dayalbagh Educational Institute, Dayalbagh, Agra 282005
[2]Department of Pharmacy, Institute of Basic Science, Dr BR Ambedkar University, Khandari Campus, Agra 282005
[3]Division of Process and Medicinal Chemistry, CSIR-CDRI, Sitapur Road, Lucknow 226031
Corresponding Author: kumar.surat@gmail.com
Received 24 November 2019; Accepted 28 December 2019

Abstract: Interactions of three synthetic β-carboline derivatives (compound A, compound B and compound C) with three nucleic acids (CT-DNA, y-RNA and t-RNA) have been investigated in the presence and absence of gold nanoparticles (AuNPs) using fluorescence quenching method and molecular docking studies. The obtained results were suggested that all the studied compounds showed the intercalative mode of binding with all nucleic acids in both the conditions. The estimated binding constant values were in the range of 10^5-10^7 M^{-1} in the absence of gold nanoparticles while in the presence of AuNPs, binding constant values were found to be in the range of 10^4-10^6 M^{-1}. Among all the complexes in both the conditions compound B showed a relatively strong binding affinity with CT-DNA. Molecular docking results indicated that the hydrogen bonds and Van der Waals interactions have a major role in the complexation to the DNA oligomers. From the molecular docking studies, it was also found that all the compounds showed the highest binding affinity with GC rich instead of AT-rich DNA. From all the above observations, it was found that all the plausible interactions occur through the intercalation mode.

Keywords: Synthetic β-carbolines derivatives, AuNps, Drug-DNA interactions, fluorescence and molecular docking

Introduction

A β-carboline prototype containing natural products and synthetic molecules have been reported Q1QAZ for their diverse biological activities. These activities include antioxidative, sedative, hypnotic, anticonvulsant, antiviral, antiparasitic, antimicrobial, anxiolytic, antileishmanial, antifungal as well as antitumor activities [1-7]. They have recently drawn the attention of the researchers due to their antitumour activities. These compounds inhibit the activity of Topisomerase and Cyclin-Dependent Kinase (CDK) etc. They also

showed intercalative mode of binding with DNA. Impressed by the biological activities of natural β-carboline alkaloids such as harmine, harmane, harmaline etc., scientists have designed synthetic β-carboline derivatives. It has been described that tetrahydro-β-carboline-tetrazole hybrids behaved as powerful anti-leishmanial agents [8-10] and might show other biological activities as well.

Natural β-carboline drugs show various pharmacological activities but in order to increase their efficacy, several research groups have focused to develop synthetic derivatives of β-carboline. These synthetic derivatives [Fig. 1] were synthesized by the chemical alteration of compounds by introducing a chemical moiety. An array of 9-substituted β-carboline derivatives were synthesized from the preliminary material harmine and L-tryptophan, respectively [11 & 12].

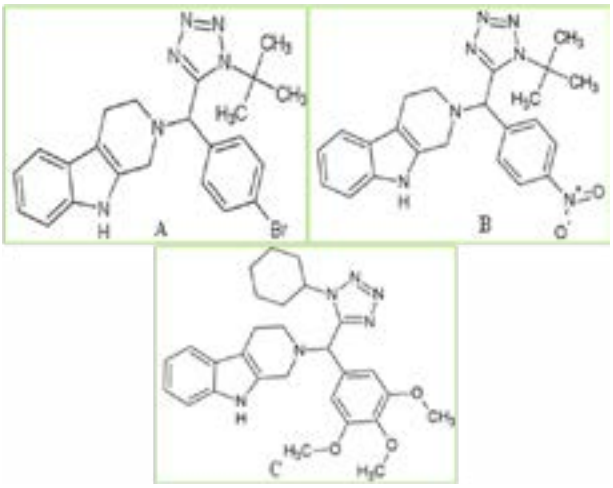

Fig. 1: Synthetic β-carboline derivatives
1A. 2-(4-Bromophenyl-1-tert-butyl-1H-tetrazol-5-yl-methyl)-2,3,4,9-tetrahydro-1H-pyrido[3,4-b]indole;
1B. 2-(1-tert-Butyl-1H-tetrazol-5-yl-4-nitrophenyl-methyl)-2,3,4,9-tetrahydro-1H-pyrido[3,4-b]indole;
1C. 2-(1-Cyclohexyl-1H-tetrazol-5-yl-3,4,5-trimethoxyphenyl-methyl)-2,3,4,9-tetrahydro-1H-pyrido[3,4-b]indole.

Suitable substituents at both position-9 and 3 of β-carboline derivatives might have a vital role in determining their improved antitumor activities and decreased acute toxicities and neurotoxic effects [13 and 14]. The substitution leads to the β-carboline derivatives having the potential as an antitumor drug**.** The biological data has also revealed that most of the synthetic derivatives of β-carboline were identified as potent anti-leishmanial agents [10].

In the present study, the molecular interactions of synthetic β-carboline derivatives with nucleic acids viz. CT-DNA, y-RNA and t-RNA were examined using fluorescence spectrophotometer. Inspired, by the nanoscience, it was decided to work on nucleic acid labelled gold nanoparticles (AuNPs) also. The binding affinities of these compounds were observed and their binding constants were calculated in the presence and absence of AuNPs. The DNA binding studies are also useful in drug designing and synthesis of new compounds with enhanced biological properties. It may further shed light on the efficient delivery of these drug molecules in the presence of AuNPs.

Materials Required

Sample Preparation

CT-DNA solution was prepared by dissolving small fragment of CT-DNA in phosphate buffer of pH 7. RNA stock solutions were prepared by dissolving in water. The concentrations of prepared CT-DNA, y-RNA, t-RNA samples were determined spectrometrically by using molar extinction coefficient (ε) values 6600, 7800 and 6900 respectively. Drugs (compound A, compound B and compound C) of 50 μM were prepared by dissolving in a suitable solvent.

Instrumentation

UV-Vis Spectrophotometer

It has provided information regarding the absorption peak of gold nanoparticles. Gold nanoparticles exhibit an optical feature generally referred to as Surface Plasmon Resonance (SPR) [15-17]. SPR of gold nanoparticles is dependent on both the shape and size of gold nanoparticles, which results in a strong absorbance band in the visible region (500 nm - 600 nm). The wavelength of absorbance peak increased with particle diameter and uneven particle shape, which was measured by Agilent Cary UV-Vis spectrophotometer. Due to the alteration in the shape, morphology and particle size, the wavelength shift significantly into the far-red region of the spectrum when compared to a spherical particle of the same diameter [18-20].

X-Ray Diffractometer

XRD pattern of gold nanoparticles was recorded using X-ray diffractometer (Bruker AXS D8 Advance, Germany) consuming Cu-kα radiation (λmax=1.54 Å) at 40 kV and 30 mA to determine crystallographic information. X-ray diffractograms of nanomaterials deliver a profusion of information from phase composition to crystallite size and lattice strain of crystallographic orientation [21]. This technique is based on Bragg's Law which depicts the relationship among the diffraction angle, the lattice spacing and the wavelength of electromagnetic radiation [22-28].

Fluorescence Spectrophotometer

Fluorescence spectroscopy is a sensitive method to study the drug-nucleic acid interactions in solution. The change in the fluorescence emission spectrum of the drug on binding with nucleic acid is used to determine the drug-nucleic acid interactions. Quantitative measurements of the binding of drugs with nucleic acids were accomplished from the fluorescence spectroscopic studies using CARY Eclipse Fluorescence Spectrophotometer [29-31].

Procedure

Preparation of Gold Nanoparticles (AuNPs)

Citrate capped gold nanoparticles were prepared by Turkevich method. The synthesized citrate-capped Au nanoparticles performed the dual function of a reducing agent as well as a stabilizer. Gold ions were reduced in gold atoms by citrate anions and stabilized colloidal AuNPs were obtained [33-38]. The obtained AuNPs were stored in the refrigerator at 4 ^{0}C till required. Gold nanoparticles were characterized by XRD and UV-Vis Spectroscopy. The concentration of AuNPs was determined using UV-Visible spectroscopy with a characteristic absorbance peak at 527 nm.

DNA-Labelled Gold Nanoparticles

Citrate capped AuNPs were labelled with an appropriate amount of nucleic acid. The solution of nucleic acid was prepared in phosphate buffer at pH 7.4 and the nucleic acid concentration was determined spectrophotometrically by using the molar extinction coefficient. The prepared AuNPs was then diluted and added to the nucleic acid solution. It was stirred vigorously and was further used for monitoring the nucleic acid–drug interactions [39-41].

Evaluation of DNA–Labelled Gold Nanoparticles

The nucleic acid-labelled AuNPs were evaluated by using UV-visible spectrometer. The pristine DNA and RNA showed absorbance peak at 260 nm, while AuNPs revealed a peak at 527 nm. On the formation of nucleic acid-labelled AuNPs, there were hypochromic and bathochromic

effects observed in the absorption wavelength of nucleic acid and gold nanoparticles respectively [42-46].

Molecular Docking Studies

Molecular docking studies were carried out with the AutoDock version 4.2 software. The crystal structures of DNA 1 and DNA 2 (PDB 4BZV and PDB 1G3X) were obtained from Protein Data Bank (http://www.rcsb.org/pdb). The 3D structure of drugs was constructed by ACD Labs Freeware ChemSketch and BIOVIA Discovery Studio. All the hydrogen atoms and Gasteiger charges were added with the help of Autodock tools. Full grid size was set to 120x120x120 for X-, Y- and Z-axes, respectively. Other necessary parameters were allotted to the default values by Autodock program. After the course of docking procedure, most favolurable configurations were generated [47-52].

Result and Discussion

Characterization of Gold Nanoparticles

Gold nanoparticles were characterized by XRD and UV-Vis Spectroscopy.

UV-Vis Spectroscopy

Evaluation of Nucleic Acid–Labelled Gold Nanoparticles: The nucleic acid-labelled AuNPs were evaluated by using UV-visible spectrophotometer. As shown [Fig. 2], AuNPs had given its characteristic peak at 527 nm which had further increased and shifted to 530 nm after the labelling with the nucleic acid. In addition to it, the nucleic acid peak was shifted from 260 nm to 256 nm after labelling with AuNPs. All the above hypochromic and bathochromic shifts confirm the labelling of nucleic acid with AuNPs.

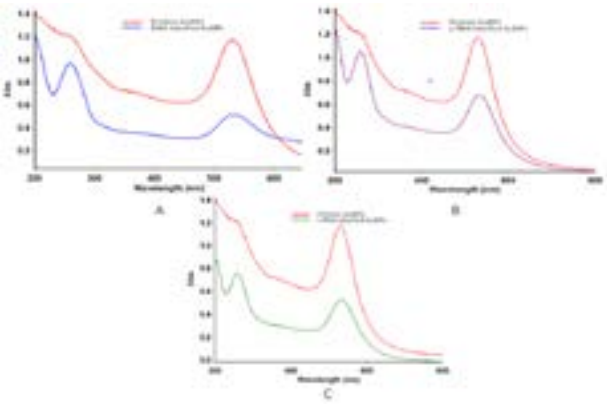

Fig. 2: UV-Vis spectra of nucleic acids labelled AuNPs; A) CT-DN-labelled AuNPs; B) yeast-RNA-labelled AuNPs; C) transfer-RNA-labelled AuNPS

XRD

X-ray diffraction (XRD) is a powerful and primary tool for examining the structure and average size of nanomaterial. In this technique, the crystalline atoms cause a beam of X-rays to diffract due to many specific planes and directions. A complete analysis of these planes and directions can produce a 3-D picture of the density of electrons within the crystal. The presence of a peak at 38.1 and 44.3 corresponds to (111) and (200) plane of gold nanoparticles as shown in Fig. 3.

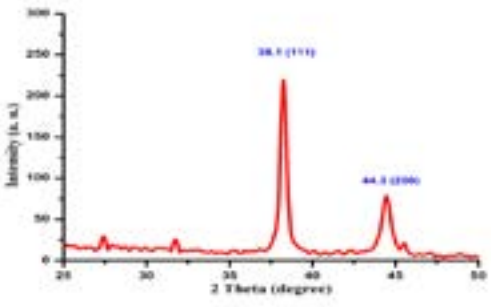

Fig. 3: XRD of gold nanoparticles

The particle size of gold nanoparticles was in the range of 30 nm.

Study of Drug-Nucleic Acid Interactions in the Absence and Presence of Gold Nanoparticles Using Fluorescence Studies

Fluorescence technique was selected for studying drug-nucleic acid interactions. In the present piece of work, the fluorescence studies were performed by taking a fixed concentration of compounds with increasing concentration of nucleic acid in the fluorescence free quartz cuvette of 1 cm path length. The excitation and emission bandpass was 5 nm each. Consistent quenching was observed among all titrations which clearly indicated that compound under study binds with the nucleic acid. The quenching data obtained from titrations were analyzed by a double reciprocal method for the evaluation of binding constants by drawing double reciprocal plot between 1/[Nucleic Acid] vs 1/[E_0-E]. Where E_0 is the initial emission maximum, while E is the emission maximum after each addition of nucleic acid aliquots). A straight line was obtained in each case and the ratio of intercept to the slope was used for calculating binding constant. This method was useful in the case of non-specific ligand interactions with the nucleic acid.

In the Absence of Gold Nanoparticles

The fixed concentration of drugs was titrated with increasing concentration of pristine nucleic acid and the hypochromic effect was observed which confirmed the interaction of all drugs with all nucleic acids. It was observed that the fluorescence intensity decreases with the increasing amount of nucleic acid. Firstly, in the initial addition of nucleic acid, large quenching of emission pattern was observed but as the amount of nucleic acid increased the quenching rate of emission peak decreased. The titrations of all the compounds (A-C) were carried out until quenching of 10% of initial emission was observed.

In the present work, the fluorescence emission spectra were measured at room temperature at pH 7.5 and concentration of drugs. To obtain the emission peak, the solution of compound A, compound B and compound C were excited at 280 nm, 285 nm and 282 nm respectively and the emission maxima were observed at 357 nm, 324 nm and 364 nm respectively. The nucleic acid aliquots from 5 µl to 50 µl were added in drug solution for three different sets of experiments.

β - Carboline Derivatives: Nucleic Acid Complex

After the analysis of fluorescence, it was found that the fluorescence intensity of drugs (Compound A-C) decreased with increasing concentration of nucleic acid. The quenching pattern of initial emission is indicated by the arrow as shown [Fig. 4 A, 5 A & 6 A]. The value of binding constant was calculated using double reciprocal plot between 1/ [nucleic acid] vs 1/ [E_O-E] [Fig. 4 B, 5 B & 6 B].

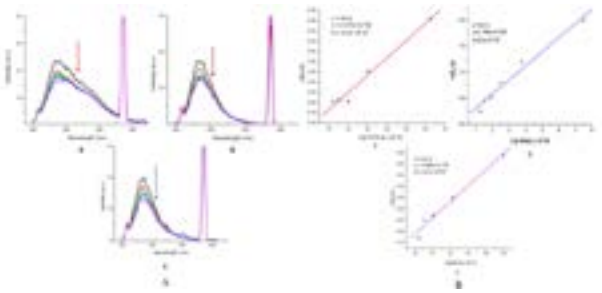

Fig. 4: A) Fluorescence emission spectra of (a) Compound A with CT-DNA, (b) Compound A with yeast-RNA, (c) Compound A with transfer-RNA; B) Double reciprocal plot of Compound A (a) with CT-DNA, b) with yeast-RNA, c) with transfer-RNA

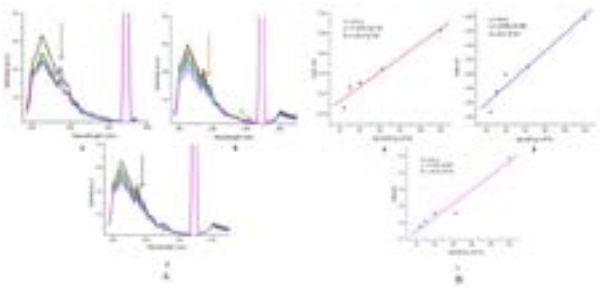

Fig. 5: A) Fluorescence emission spectra of (a) Compound B with CT-DNA, (b) Compound B with yeast-RNA, (c) Compound B with transfer-RNA; B) Double reciprocal plot of Compound B (a) with CT-DNA, b) with yeast-RNA, c) with transfer-RNA

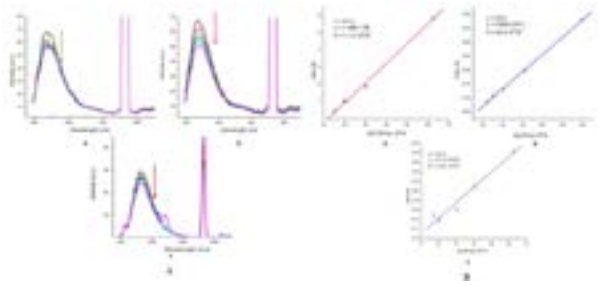

Fig. 6: A) Fluorescence emission spectra of (a) Compound C with CT-DNA, (b) Compound C with yeast-RNA, (c) Compound C with transfer-RNA; B) Double reciprocal plot of Compound C (a) with CT-DNA, b) with yeast-RNA, c) with transfer-RNA

Table 1: Binding constant values of Compound A, Compound B and Compound C with all the nucleic acids (CT-DNA, y-RNA sand t-RNA) in the absence of AuNPs

Complex	Binding Constant (M^{-1})
Compound A: CT-DNA	4.5×10^6
Compound A: y-RNA	9.2×10^5
Compound A: t-RNA	3.3×10^6
Compound B: CT-DNA	1.6×10^7
Compound B: y-RNA	6.1×10^6
Compound B: t-RNA	1.6×10^6
Compound C: CT-DNA	1.1×10^6
Compound C: y-RNA	3.6×10^5
Compound C: t-RNA	1.5×10^5

The calculated binding constant for compounds A-C with all the nucleic acids were estimated in the range of 10^5-10^7 M^{-1} (Table 1). It revealed that all drugs showed complementary binding with all nucleic acids. All the Compounds showed the prominent binding with CT- DNA as compared to y-RNA and t-RNA. Among all the complexes in the absence of AuNPs, it was found that compound B showed strong binding with CT-DNA and compound C showed poor binding with t-RNA. The calculation of binding constants was also carried out to determine the plausible order of binding among all the complexes in the absence of AuNPs as noted below:

Compound B : CT-DNA > Compound B : y-RNA > Compound A : CT-DNA > Compound A : t-RNA > Compound B : t-RNA > Compound C : CT-DNA > Compound A : y-RNA > Compound C : y-RNA > Compound C : t-RNA

In the Presence of AuNPs

The fixed concentrations of drugs were excited on their corresponding wavelengths and showed their characteristic emission maxima as discussed earlier after the addition of aliquots of nucleic acid labelled AuNPs measuring from 5 µl to 50 µl. It was found that the fluorescence intensity decreased with increasing concentration of nucleic acid marked by an arrow [Fig. 7 A, 8 A & 9 A]. The value of binding constant was calculated using double reciprocal plot between 1/[AuNPs-nucleic acid] vs $1/[E_O-E]$ [Fig. 7 B, 8 B & 9 B].

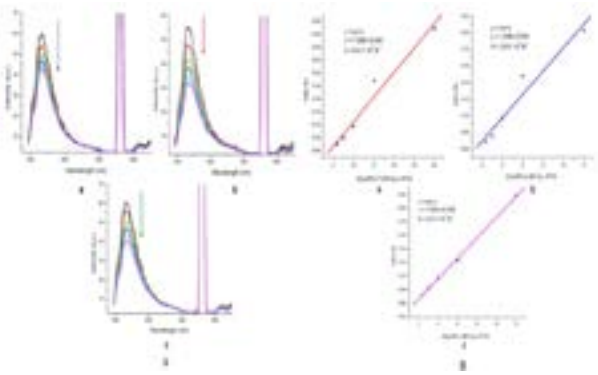

Fig. 7: A) Fluorescence emission spectra of (a) Compound A with CT-DNA labelled AuNPS, (b) Compound A with yeast-RNA labelled AuNPs, (c) Compound A with transfer-RNA labelled AuNPs; B) Double reciprocal plot of Compound A (a) with CT-DNA labelled AuNPs, (b) with yeast-RNA labelled AuNPs, (c) with transfer-RNA labelled AuNPs

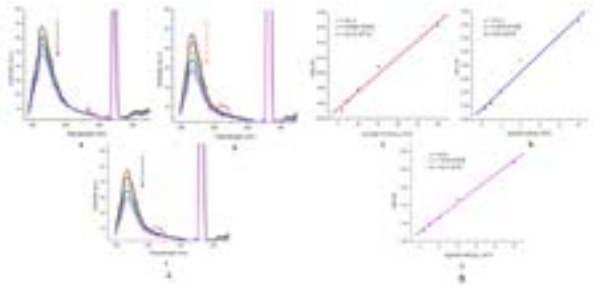

Fig. 8: A) Fluorescence emission spectra of (a) Compound B with CT-DNA labelled AuNPS, (b) Compound B with yeast-RNA labelled AuNPs, (c) Compound B with transfer-RNA labelled AuNPs; B) Double reciprocal plot of Compound B (a) with CT-DNA labelled AuNPs, (b) with yeast-RNA labelled AuNPs, (c) with transfer-RNA labelled AuNPs

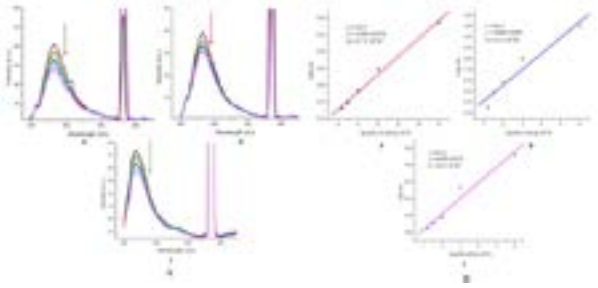

Fig. 9: A) Fluorescence emission spectra of (a) Compound C with CT-DNA labelled AuNPS, (b) Compound C with yeast-RNA labelled AuNPs, (c) Compound C with transfer-RNA labelled AuNPs; B) Double reciprocal plot of Compound C (a) with CT-DNA labelled AuNPs, (b) with yeast-RNA labelled AuNPs, (c) with transfer-RNA labelled AuNPs

Table 2: Binding constant values of Compound A, Compound B and Compound C with all the nucleic acids (CT-DNA, y-RNA and t-RNA) in the presence of AuNPs

Complex	Binding Constant (M^{-1})
Compound A:AuNPs-CT-DNA	$6.4 \times 10^5 M^{-1}$
Compound A:AuNPs-y-RNA	$2.9 \times 10^6 M^{-1}$
Compound A:AuNPs-t-RNA	$2.3 \times 10^5 M^{-1}$
Compound B:AuNPs-CT-DNA	$6.5 \times 10^6 M^{-1}$
Compound B:AuNPs-y-RNA	$5.8 \times 10^4 M^{-1}$
Compound B:AuNPs-t-RNA	$8.0 \times 10^4 M^{-1}$
Compound C:AuNPs-CT-DNA	$1.2 \times 10^5 M^{-1}$
Compound C:AuNPs-y-RNA	$3.1 \times 10^5 M^{-1}$
Compound C:AuNPs-t-RNA	$2.5 \times 10^4 M^{-1}$

On the assessment of the binding constant values in the presence of AuNPs for compounds A-C with all the nucleic acids (CT-DNA, y-RNA and t-RNA) it was found that all the compounds showed the binding in the range to $10^4 – 10^6 M^{-1}$. From Table 2, it revealed that in the presence

of AuNPs compound B showed the maximum binding affinity with CT-DNA and compound C showed minimum binding affinity with t-RNA. The estimated order of binding in the presence of nucleic acid is summarized below:

Compound B : AuNPs-CT-DNA > Compound A : AuNPs-y-RNA > Compound A : AuNPs-CT-DNA > Compound C : AuNPs-y-RNA > Compound A : AuNPs-t-RNA > Compound C : AuNPs-CT-DNA > Compound B : AuNPs-t-RNA > Compound B : AuNPs-y-RNA > Compound C : AuNPs-t-RNA

Table 3: Comparative Binding Constant Values of β-Carboline Derivatives in the Absence and Presence of Gold Nanoparticles (AuNPs)

Complexes	Nucleic Acid	In the Absence of AuNPs	In the Presence of AuNPs
Compound A	CT-DNA	$4.5 \times 10^6\ M^{-1}$	$6.4 \times 10^5\ M^{-1}$
Compound B		$1.6 \times 10^7\ M^{-1}$	$6.5 \times 10^6\ M^{-1}$
Compound C		$1.1 \times 10^6\ M^{-1}$	$1.2 \times 10^5\ M^{-1}$
Compound A	y-RNA	$9.2 \times 10^5\ M^{-1}$	$2.9 \times 10^6\ M^{-1}$
Compound B		$6.1 \times 10^6\ M^{-1}$	$5.8 \times 10^4\ M^{-1}$
Compound C		$3.6 \times 10^5\ M^{-1}$	$3.1 \times 10^5\ M^{-1}$
Compound A	t-RNA	$3.3 \times 10^6\ M^{-1}$	$2.3 \times 10^5\ M^{-1}$
Compound B		$1.6 \times 10^6\ M^{-1}$	$8.0 \times 10^4\ M^{-1}$
Compound C		$1.5 \times 10^5\ M^{-1}$	$2.5 \times 10^4\ M^{-1}$

On comparing the binding constant values of Compounds A-C with all the nucleic acids (CT-DNA, y-RNA and t-RNA) in the presence and absence of AuNPs it was observed that among all 18 complexes the highest binding affinity was shown by compound B with CT-DNA (Table 3).

Molecular Docking Studies

Molecular docking method provides some insight into drug-DNA interactions by generating structure scaffold of the drug-DNA complexes. It can also contribute to mechanistic studies by inserting a drug into specific DNA binding sites.

In the present study, the molecular docking was performed to analyze the binding site information and the comparative efficiency of binding among the three β-carboline derivatives (A-C) with GC-rich and AT-rich DNA. In each docking, the 10 most complimentary structures were analyzed, in all the performed 20 runs. The planar ring segment of drug structure was intercalated in the cavity of DNA sequences [Fig. 10 A & 10 B]. Examination of docking was clearly indicated that all the derivatives showed intercalation mode of binding instead of the groove binding. Results also suggested that Van der Waals, electrostatic and certain hydrogen-bonds (Table IV) facilitated the favoured binding modes among complexes of drugs and DNA.

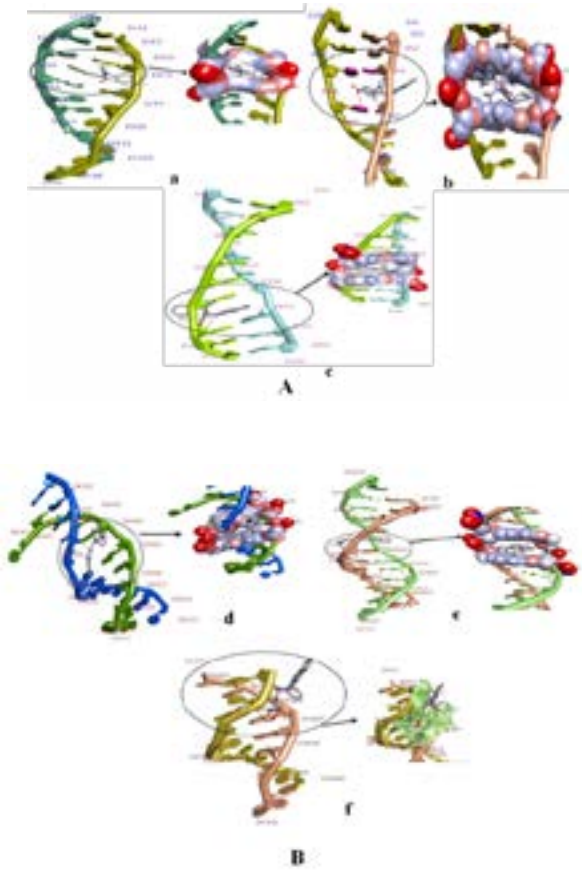

Fig. 10: A) β-carboline derivatives binding with intercalation cavity of duplex DNA; B) β-carboline derivatives binding with intercalation cavity of duplex DNA.

The energetically favoured confirmations clearly indicate that all drugs fit into the GC rich cavity [Fig. 10 A & 10 B]. While in the case AT-rich cavity compound A and compound C approach towards DNA minor groove instead of intercalation cavity. Thus, it concluded that there is complementary base specific DNA binding with drugs.

Table 4: Calculated Binding Energy and Binding Constant for All Three β-Carbolines:DNA Complexes from Docking Method

Complexes	Binding Energy ($\Delta G_{theoretical}$)	Binding Constant ($K_{theoretical}$)	Hydrogen Bonds
Compound A : DNA1	-7.60	$3.92x10^5$	G3H7:Drug N17
Compound B : DNA 1	-6.59	$1.19x10^5$	G3H7:Drug N17, G15H7:Drug O27
Compound C : DNA 1	-6.33	$4.52x10^4$	G6H3:Drug N17, N19
Compound A : DNA 2	-6.47	$5.75x10^4$	G3H2:Drug N9
Compound B : DNA 2	-5.13	$5.94x10^3$	G12H3:Drug O27
Compound C : DNA 2	-4.63	$2.8x10^3$	G16H3:Drug O27

Furthermore, the theoretical binding energy and binding constants (Table 4) concluded that all the compounds (A-C) showed the highest binding with GC rich instead of AT-rich DNA. It was also noticed that compound A and compound C possess the excellent binding with GC rich cavity among other complexes. Theoretical binding constant (10^3-10^5) values were different from experimental values (10^5-10^7). For the theoretical complexes, the plausible binding sites for DNA 1 (i.e. GC rich cavity) with all three compounds (A-C) are G3H7:Drug N17, G3H7:Drug N17, G15H7:Drug O27 and G6H3:Drug N17, N19 respectively and for DNA 2 (i.e. AT rich cavity) with all three compounds (A-C) are G3H2:Drug N9, G12H3:Drug O27 and G16H3:Drug O27 respectively. The conformations obtained after runs Autodock clearly indicate the formation of hydrogen bonding with H, O and N atoms of β-carboline derivatives. The experiment results for all the complexes are higher than the theoretical binding results. From all the above observations, it was revealed that all the β-carboline showed affinity towards GC base pairs and interacts through the intercalation mode of binding.

Conclusions

The comparative binding study of three synthetic β-carboline derivatives compound (A-C) with three nucleic acids (CT-DNA, y-RNA and t-RNA) were studied in the presence and absence of gold nanoparticles (AuNPs) by fluorescence quenching method and molecular docking studies. The decrease in the peak height of emission spectra for all the complexes in all the cases confirms the interactions between drugs and nucleic acids. The obtained binding constant values were in the range of 10^5-10^7 M^{-1} and 10^4-10^6 M^{-1} in the absence and presence of AuNPs respectively. On comparing the binding constant values in the presence and absence of AuNPs Compound B:CT-DNA complex showed the maximum interaction among all complexes. From this study, the greater binding constant in the absence of AuNPs as compared to their presence signifies the competitive binding occurred between the nucleic acids and AuNPs with drugs. Fluorescence quenching and Molecular docking studies suggested that the β-carboline derivatives plausibly interact via intercalation mode of binding and GC specificity with nucleic acids. The major forces involve in the complexations are hydrogen bonding, electrostatic and Van der Waals forces. This study provides information about the order of binding in both the cases and some information about the mechanism of action of drugs.

Acknowledgements

Surat Kumar acknowledges profound humble gratitude to Revered Prof. P. S. Satsangi Sahab, the Chairman, Advisory Committee on Education, Dayalbagh, Agra, India for the sustained inspiration and constant encouragement. Authors are thankful to Prof. P. K. Kalra, Director, Dayalbagh Educational Institute, Dayalbagh, Agra, India for providing the infrastructure and laboratory facilities. One of author Monika Yadav also acknowledges her gratitude to the University Grants Commission (UGC), New Delhi, India for providing UGC-BSR Fellowship.

Conflicts of Interest

The authors certify that they have no affiliations with or participation in any organization or entity with any financial interest

References

1. Zaker F, Oody A and Arjmand A, A study on the anti-tumoral and differentiation effects of *Peganum harmala* derivatives in combination with ATRA on leukaemic cells, *Arch. Pharmacal Res.* 2007, **30**, 844-849.
2. Egusa H, Doi M, Saeki M, Fukuyasu S, Akashi Y and Yokota Y, The small molecule harmine regulates NFATc1 and Id2 expression in osteoclast progenitor cells, *Bone*. 2011, **49**, 264-274.
3. Frost D, Meechoovet B, Wang T, Gately S, Giorgetti M and Shcherbakova I, β-carboline compounds, including harmine, inhibit DYRK1A and tau phosphorylation at multiple Alzheimer's disease-related sites, *PLoS*. 2011, **6**, e19264.
4. Hamsa TP and Kuttan G, Harmine activates intrinsic and extrinsic pathways of apoptosis in B16F-10 melanoma, *Chin. Med. J*. 2011, **6**, 11-19.
5. Onishi Y, Oishi K, Kawano Y and Yamazaki Y, The harmala alkaloid harmine is a modulator of circadian Bmal1 transcription, *Bioscience Rep*. 2012, **32**, 45-52.
6. Réus GZ, Stringari RB, Gonçalves CL, Scaini G, Carvalho-Silva M and Jeremias GC, Administration of harmine and imipramine alters creatine kinase and mitochondrial respiratory chain activities in the rat brain, *Depress. Res. Treat*. 2012, **2012**, 987397-987403.
7. Yonezawa T, Hasegawa S, Asai M, Ninomiya T, Sasaki T and Cha BY, Harmine, a β-carboline alkaloid, inhibits osteoclast differentiation and bone resorption *in vitro* and *in vivo*, *Eur. J. Pharmacol*. 2011, **650**, 511-518.
8. Li Y, Liang F, Jiang W, Yu F, Cao R, Ma Q, Dai X, Jiang J, Wang Y and Si S, DH334 a β-carboline anti-cancer drug, inhibits the CDK activity of budding yeast, *Cancer Biol Ther*. 2007, **6**, 1204-1210.
9. Nafisi S, Bonsaii M, Maali P, Khalilzadeh MA, Manouchehri F, β-carboline alkaloids bind DNA, *J. Photochem. Photobiol*. 2010, **100**, 84-91.
10. Purohit P, Pandey AK, Singh D, Chouhan PS, Ramalingam K, Shukla M, Goyal N, Lal J and Chauhan PMS, An insight into tetrahydro-β-carboline-tetrazole hybrids: Synthesis and bioevaluation as potent antileishmanial agents, *Med. Chem. Comm*. 2017, **8**, 1824-1834.
11. Al-Allaf TAK and Rashan LJ, Synthesis and cytotoxic evaluation of the first trans-palladium(II) complex with naturally occurring alkaloid harmine, *Eur. J. Med. Chem*. 1998, **33**, 817-820.
12. Akhtar R, Yousaf M, Naqvi SAR, Irfan M, Zahoor AF, Hussain AI and Chatha SAS, Synthesis of ciprofloxacin-based compounds: A review, *Synth. Commun*. 2016, **46**, 1849-1879.
13. Cao R, Chen Q, Hou X, Chen H, Guan H, Ma Y, Peng W and Xu A, Synthesis, acute toxicities and antitumor effects of novel 9-substituted β-carboline derivatives, *Bioorganic Med. Chem.* 2004, **12**, 4613-4623.
14. Marx S, Bodart L, Tumanov N and Wouters J, Design and synthesis of a new soluble natural β-carboline derivative for preclinical study by intravenous injection, *Int. J. Mol. Sci.* 2019, **20**, 1-14.
15. Manivasagan P, Bharathiraja S, Bui NQ, Jang B, Oh YO, Lim IG, Oh J, Doxorubicin-loaded fucoidan capped gold nanoparticles for drug delivery and photoacoustic imaging, *Int. J. Biol. Macromol*. 2016, **91**, 578-588.
16. Amendola V and Meneghetti M, Size evaluation of gold nanoparticles by UV-Vis Spectroscopy, *J. Phys. Chem. C*. 2009, **113**, 4277-4285.
17. Long NN, Vu LV, Kiem CD, Doanh SC, Nguyet CT, Hang PT, Thien ND and Quynh LM, Synthesis and optical properties of colloidal gold nanoparticles, *J Phys. Conf. Ser*. 2009, **187**, 1-8.
18. Singh P, Kumari K, Katyal A, Kalra R and Chandra R, Synthesis and characterization of silver and gold nanoparticles in ionic liquid, *Spectrochim. Acta A*. 2009, **73**, 218-220.
19. Parveen R, Shamsi TN and Fatima S, Nanoparticles-protein interaction: Role in protein aggregation and clinical implications, *Int. J. Biol. Macromol*. 2017, **94**, 386-395.
20. Sonia, Komal, Kukreti S and Kaus M, Exploring the DNA damaging potential of chitosan and citrate-reduced gold nanoparticles: Physicochemical approach, *Int. J. Biol. Macromol*. 2018, **115**, 801-810.

21. Yadav S, Sharma M, Gaanesh N, Srivastava S and Srivastava MM, Enhanced anti melanoma bioefficacy of flavonoid loaded gold nanoparticles for prepared from the plant *Madhuca longifolia* on the Mice and human melanoma cell lines, 2019, **8**, 833-843.
22. Singh P, Kumari K, Katyal A, Kalra R and Chandra R, Synthesis and characterization of silver and gold nanoparticles in ionic liquid, *Spectrochim. Acta A*. 2009, **73**, 218-220.
23. Dorofeeva GA, Streletskii AN, Povstugar IV, Protasov AV and Elsukov EP, Determination of nanoparticle sizes by the X-ray diffraction method, *Colloid J*. 2012, **74**, 678-688.
24. Krishnamurthy S, Esterle A, Sharma NC and Sahi SV, Yucca-derived synthesis of gold nanomaterial and their catalytic potential, *Nanoscale Res. Lett*. 2014, **9**, 1-9.
25. Ingham B, X-ray scattering characterisation of nanoparticles, *Crystallogr. Rev.* 2015, **21**, 229-303.
26. Verma A, Srivastav A, Sharma D, Banerjee A, Sharma S, Satsangi VR, Shrivastav R, Avasthi DK and Dass S, A study on the effect of low energy ion beam irradiation on Au/TiO_2 system for its application in photoelectrochemical splitting of water, *Nucl. Instr. Meth. B*. 2016, **379**, 255-261.
27. Srivastav A, Verma A, Banerjee A, Khan SA, Gupta M, Satsangi VR, Shrivastav R and Das S, Gradient doping - A case study of Ti-Fe_2O_3 towards improved photoelectrochemical response, *Phys. Chem. Chem. Phys*. 2016, **18**, 32735-32743.
28. Boddolla S, Thodeti S, A review on characterization techniques of nanomaterials, *IJESM*. 2018, **7**, 169-175.
29. Islam MM, Pandya P, Kumar S and Kumar GS, RNA targeting through binding of small molecules: Studies on t-RNA binding by the cytotoxic protoberberine alkaloid coralyne, *Mol. Bio. Syst*. 2009, **5**, 244-254.
30. Gupta SP, Pandav K, Pandya P, Kumar GS, Barthwal R and Kumar S, Methylene linker assisted DNA binding of vinblastine and simpler analogs: Purine-Pyrimidine specificity of Indole derivatives, *CBI.* 2011, **1**, 297-309.
31. Pandya P, Gupta SP, Pandav K, Barthwal R, Jayaram B and Kumar S, DNA binding studies of vinca alkaloids: Experimental and computational evidence, *NPC*. 2012, **7**, 1-6.
32. Yadav M, Gupta SP and Kumar S, Spectroscopic and electrochemical studies of vinblastine with yeast-RNA (y-RNA) and transfer-RNA (t-RNA), 2017, 73-79, ISBN:978-93-86439-23-9.
33. Turkevich J, Stevenson PC, Hillier J, A study of the nucleation and growth processes in the synthesis of colloidal gold, *Discuss*. *Faraday Soc.* 1951, **11**, 5-75.
34. Frens G, Controlled nucleation for the regulation of the particle size in monodisperse gold suspensions, *Nature Phys. Sci*. 1973, **241**, 20-22.
35. Kimling J, Maier M, Okenve B, Kotaidis V, Ballot H, and Plech A, Turkevich method for gold nanoparticle synthesis revisited, *J. Phys. Chem. B*. 2006, **110**, 15700-15707.
36. Jingyue ZHAO and Bernd F, Synthesis of gold nanoparticles via chemical reduction method, *International Conference on Nanotechnology* (NANOCON), 2015, 1-7.
37. Freitas de Freitas L, Varca GHC, Dos Santos Batista JG and Benévolo Lugão A, An overview of the synthesis of gold nanoparticles using radiation technologies, *Nanomaterials*. 2018, **8**, 1-23.
38. Sun L, Pu S, Li J, Cai J, Zhou B, Ren G, Ma Q, Zhong L, Size controllable one step synthesis of gold nanoparticles using carboxymethyl chitosan, *Int. J. Biol. Macromol.* 2019, **122**, 770-783.
39. Lad AKN and Agrawal YK, DNA-labeled gold-based optical nanobiosensor monitoring DNA–mitoxantrone interaction, *BioNanoScience*. 2012, **2**, 9-15.
40. Lad AKN and Agrawal YK, Optical nanobiosensor: A new analytical tool for monitoring carboplatin-DNA interactionin vitro, *Talanta*. 2012, **97**, 218-221.
41. Lad AKN and Agrawal YK, SiO_2-based nanobiosensor monitoring toxicological behavior of mitoxantrone in vitro, *Appl Nanosci*. 2014, **4**, 523-529.
42. Demers LM, Mirkin CA, Mucic RC, Reynolds RA, Letsinger, RL, Elghanian R, and Viswanadham G, A fluorescence-based method for determining the surface coverage and hybridization efficiency of thiol-capped oligonucleotides bound to gold thin films and nanoparticles. *Anal. Chem*. 2002, **72**, 5535-5541.
43. You CC, Chompoosor A, Rotello VM, The biomacromolecule-nanoparticle interface, *Nanotoday*. 2007, **2**, 34-43.
44. Jiang G, Wang L, Chen W, Studies on the preparation and characterization of gold nanoparticles protected by dendrons, *Mater. Lett*. 2007, **61**, 278-283.
45. Qiao FY, Liu J, Li FR, Kong XL, Zhang HL, Zhou HX, Antibody and DNA dual-labeled gold nanoparticles: Stability and reactivity, *Appl Surf Sci.* 2008, **254**, 2941-2946.
46. Perfezou M, Turner A and Merkoci A, Cancer detection using nanoparticle-based sensors, *Chem. Soc. Rev*. 2012, **41**, 2606-2622.
47. Feroz SR, Mohamad SB, Bujang N, Malek SNA, and Tayyab S, Multispectroscopic and molecular modeling approach to investigate the interaction of flavokawain B with human serum albumin, *J. Agric. Food Chem*. 2012, **60**, 5899-5908.
48. Chai J, Wang J, Xu Q, Hao F and Liu R, Multi-spectroscopic methods combined with molecular modeling dissect the interaction mechanisms of ractopamine and calf thymus DNA, *Mol. BioSyst*. 2012, **8**, 1902-1907.
49. Li XL, Hu YJ, Wang H, Yu BQ, and Yue HL, Molecular spectroscopy evidence of berberine binding to DNA: Comparative binding and thermodynamic profile of intercalation, *Biomacromolecules*. 2012, **13**, 873-880.
50. Sharma S, Yadav M, Gupta PS, Pandav K and Kumar S, Spectroscopic and structural studies on the interaction of

an anticancer β–carboline alkaloid, harmine with GC and AT specific DNA oligonucleotids, *Chem.-Biol. Interact.* 2016, **260**, 256-262.

51. Sharma S, Gupta SP, Pandav K and Kumar S, Spectroscopic and molecular docking studies on the interaction of an anticancer β-carboline alkaloid, harmine with GC and AT specific DNA oligonucleotides, *CBI*. 2016, **6**, 126-136.
52. Yang Y, Zhang N, Sun Y, Li J, Zhao R, Zheng Z, Ding Y, Zhang X, Geng D and Sun Y, Multispectroscopic and molecular modeling studies on the interaction of bile acids with Bovine Serum Albumin (BSA), *J. Mol. Struct*. 2019, **1180**, 89-99.